23rd International Conference on Renewable Energies and Power Quality (ICREPQ'25)
Tenerife (Spain), 25th to 27th June 2025
Renewable Energy and Power Quality Journal (RE&PQJ)
ISSN 2172-038 X, Volume No.23, September 2025

Assessment and thermal modeling of the impact of a floating photovoltaic system on lake temperature

K. Sredenšek[1,2], D. Kuhar[1], J. Počivalnik[1], E. Simonič[1], G. Štumberger[2] and S. Seme[1,2]

[1] Faculty of Energy Technology, University of Maribor
Hočevarjev trg 1, 8270 Krško, Slovenia
e-mail: klemen.sredensek@um.si; domen.kuhar@um.si; jernej.pocivalnik@um.si; eva.simonic@um.si; sebastijan.seme@um.si

[2] Faculty of Electrical Engineering and Computer Science, University of Maribor
Koroška cesta 46, 2000 Maribor, Slovenia
e-mail: gorazd.stumberger@um.si

Abstract. This paper evaluates the impact of a floating photovoltaic system on lake temperature using a one-dimensional thermal model. The modeling approach incorporates established heat flux formulations and lake temperature dynamics, utilizing key meteorological inputs such as power density of solar radiation, wind speed, air temperature, humidity, and precipitation. The model analyzes temperature variations at different depths under various floating photovoltaic system coverage scenarios and compares them to a reference case without a floating photovoltaic system. The results indicate that a floating photovoltaic system affects the lake's thermal regime by enhancing cooling during warmer months and limiting heat loss in colder periods. A floating photovoltaic system also alters latent heat flux and evaporation, further affecting the lake's energy balance and stratification. These findings highlight the importance of considering FPV-related thermal effects in environmental assessments.

Key words. floating photovoltaic system, thermal modeling, lake temperature, one-dimensional model

1. Introduction

In recent years, photovoltaic (PV) systems have been predominantly installed on rooftops, degraded land, agricultural areas, and other available surfaces. Due to spatial constraints, European regulations have facilitated the deployment of PV systems on water bodies. However, each installation must undergo a thorough environmental impact assessment. In Slovenia, a key regulatory requirement is determining whether a floating photovoltaic (FPV) system significantly restricts space or leads to environmental degradation. One crucial aspect of this evaluation is understanding its impact on lake temperature.
Various papers have explored different approaches for modeling lake temperature distribution. Wang et al. [1] applied a one-dimensional (1D) model to simulate thermal stratification in Lake Qiandaohu, refining parameterization with time-dependent light extinction coefficients and eddy diffusivity. Similarly, Šarović et al. [2] developed a 1D energy budget model for predicting vertical temperature profiles in warm, monomictic lakes, demonstrating its applicability for both short- and long-term simulations, albeit with slight overestimations in epilimnion temperature and thermocline thickness. Gaillard et al. [3] expanded the use of 1D models by evaluating a multi-column lake model (MCM) for Lake Geneva, offering a computationally efficient alternative to full three-dimensional (3D) hydrodynamic models. Additionally, Gu et al. [4] and Tasnim et al. [5] compared 1D and 3D modeling approaches, highlighting their respective strengths and limitations in simulating water temperature, ice cover, and dissolved oxygen dynamics. While these papers have refined methods for modeling lake temperature distribution, recent research has increasingly focused on understanding how FPV systems influence lake thermal dynamics.
Several studies have examined the thermal impact of FPV using different modeling techniques and field measurements. Exley et al. [6] used the 1D MyLake model to show that FPV generally lowers surface temperatures, shortens stratification, and reduces mixing depth, though effects vary with system design and coverage. Similarly, Liu et al. [7] found that FPV reduces daytime water temperatures but retains heat at night, weakening diurnal fluctuations and modifying local microclimate conditions. Ilgen et al. [8] confirmed these findings through field measurements, showing that FPV can cool upper water layers by up to 2.8 °C, particularly during the day. Yang et al. [9] and Rahaman et al. [10] highlighted the role of radiation balance in FPV systems. Yang et al. [9] observed that FPV reduces shortwave radiation while increasing longwave radiation, leading to heat retention beneath the PV modules. This was further supported by Yang et al. [11], who found that FPV can increase water temperature under the PV modules by 0.3 °C while simultaneously stabilizing the water column and reducing mixing energy.
These papers collectively demonstrate that FPV influences lake temperature, stratification, and energy balance, with effects highly dependent on system design,

coverage, and local environmental conditions. While FPV typically cools surface waters, localized warming beneath the PV modules has also been observed, highlighting the complex and site-specific nature of FPV impacts. Building upon these findings, this paper presents a modified 1D modeling approach that integrates different modeling techniques to assess the thermal effects of FPV on lake conditions. The results of the 1D model will be presented using a lake in Slovenia as a case study, focusing on temperature variations with and without an FPV system. Other authors have previously evaluated the model used in this paper, confirming its applicability for simulating lake thermal dynamics under various environmental conditions.

2. Methodology

In this paper, a 1D model, previously analyzed by other authors [2, 4, 5, 7, 9], was employed to simulate the temperature distribution of the lake. Subsurface energy transport is governed by the 1D heat diffusion equation [2], expressed by (1):

$$c_{\mathrm{p}}\rho\frac{\partial T}{\partial t}=\frac{\partial}{\partial z}\left\{\left[k_m+k_t\right]\frac{\partial T}{\partial z}\right\}-\frac{\partial \phi}{\partial z} \tag{1}$$

Where T represents the lake temperature (K), k_{m} and k_{t} denote the molecular and turbulent thermal conductivity ($\mathrm{Wm^{-1}K^{-1}}$), ρ is the water density ($\mathrm{kg\ m^{-3}}$), t stands for time (s), z represents depth (m), C_{p} is the specific heat capacity of water ($\mathrm{J\ kg^{-1}K^{-1}}$) and ϕ denotes the heat flux ($\mathrm{W/m^2}$). The water density ρ is calculated using an empirical equation dependent on temperature and is given by (2):

$$\begin{aligned}\rho = {} & 999.8395+6.7914\cdot10^{-2}T-9.0894\cdot10^{-3}T^2+\\ & 1.0171\cdot10^{-4}T^3-1.2846\cdot10^{-6}T^4+1.1592\cdot10^{-8}T^5-\\ & 5.0125\cdot10^{-11}T^6\end{aligned} \tag{2}$$

The turbulent thermal conductivity k_{t} is expressed as a function of time and depth in equation (3), as it is influenced by meteorological forcing.

$$k_{\mathrm{t}}\left(z\right)=c_{\mathrm{p}}\rho\left(\frac{ku^*z}{\mathrm{Pr}_0}\right)\exp\left(-k^*z\right)\left(1+37R_{\mathrm{i}}^2\right)^{-1} \tag{3}$$

Where u^* represents the friction velocity at the surface ($\mathrm{m\cdot s^{-1}}$), k = 0,4 is the von Kármán constant, k^* is the latitude-dependent parameter of the Ekman profile, R_{i} denotes the Richardson number, and Pr_0 = 1 is the neutral value of the turbulent Prandtl number. The parameter of the Ekman profile is defined by (4):

$$k^*=6.6\left(\sin\varphi\right)^{1/2}U_2{}^{-1.84} \tag{4}$$

Where U_2 represents the wind speed at a height of 2 m, and φ denotes the latitude of the observed lake. The Richardson number is calculated using (5):

$$Ri=\frac{-1+\left\{1+40N^2k^2z^2/\left[u^{*^2}\exp\left(-2k^*z\right)\right]\right\}^{1/2}}{20} \tag{5}$$

Where N denotes the Brunt-Väisälä frequency ($\mathrm{s^{-1}}$) and is presented by (6):

$$N=\left[-g/\rho\left(\partial\rho/\partial z\right)\right]^{1/2} \tag{6}$$

The friction velocity u^* at the surface is calculated through wind speed by (7):

$$u^*=\frac{U_2\cdot k}{\log\left(2/z_0\right)} \tag{7}$$

The definition of heat fluxes follows, presenting the fundamental 1D heat diffusion equation. These consist of net shortwave radiation S_{n}, net longwave radiation L_{n}, latent heat flux H_{l}, sensible heat flux H_{s}, and heat flux from precipitation H_{p}. The surface net heat flux is presented by (8):

$$\phi=S_{\mathrm{n}}+L_{\mathrm{n}}+H_{\mathrm{s}}+H_{\mathrm{l}}+H_{\mathrm{p}} \tag{8}$$

Net shortwave radiation presented by (9) is primarily determined by the received power density of solar radiation at the water surface or photovoltaic modules.

$$S_{\mathrm{n}}=G\cdot\alpha_{\mathrm{s}} \tag{9}$$

Where G represents the power density of solar radiation on the observed surface, and α_{s} denotes the absorption coefficient of the surface (water or PV modules). Net longwave radiation L_{n} is defined as the balance between downward atmospheric longwave radiation and the upward emission from the lake or PV module surface and is calculated by (10):

$$L_{\mathrm{n}}=\left(1-r\right)\left[\varepsilon_{\mathrm{a}}\sigma\left(T_{\mathrm{a}}+273.15\right)^4\right]-\varepsilon\sigma\left(T_{\mathrm{s}}+273.15\right)^4 \tag{10}$$

Where ε and ε_{a} denote the emissivities of the lake surface and atmosphere, respectively, T_{a} represents the air temperature, r is the water's reflectivity for longwave radiation, T_{s} corresponds to the water surface temperature, and σ is the Stefan-Boltzmann constant. The atmospheric emissivity is influenced by the water vapor content and the temperature profile of the atmosphere and is calculated using (11).

$$\varepsilon_{\mathrm{a}}=\left(1-f\right)\varepsilon_{\mathrm{ac}}+f \tag{11}$$

Where $\varepsilon_{\mathrm{ac}}$ represents the atmospheric emissivity under clear sky conditions, and f denotes the cloud fraction. The atmospheric emissivity under clear sky conditions can be further determined using (12):

$$\varepsilon_{\mathrm{ac}}=1.24\left[e_{\mathrm{a}}/\left(T_{\mathrm{a}}+273.15\right)\right]^{1/7} \tag{12}$$

Where e_a denotes the water vapor pressure (hPa), which depends on relative humidity rh and the saturation vapor pressure e_s presented by (13):

$$e_a = e_s(T_a)\,rh \tag{13}$$

The latent H_l and sensible H_s heat fluxes are determined using the methodology described in [2] and are expressed by (14) and (15), respectively.

$$H_l = -\rho_a L_v C_E U_z (q_s - q_a) \tag{14}$$

$$H_s = -\rho_a c_a C_H U_z (T_s - T_a) \tag{15}$$

Where L_v = 2500 kJ kg^{-1} is the latent heat of evaporation, c_a represents the specific heat capacity of air, ρ_a denotes the air density (kg m^{-3}), C_E and C_H are the transfer coefficients for latent and sensible heat flux, respectively, and q_a and q_s represent the specific humidities (kg/kg^{-1}). The heat flux due to precipitation H_p is given by (16):

$$H_{prec} = 1000 \cdot C_p \cdot P \cdot (T_{air} - T) \tag{16}$$

Where C_p represents the specific heat capacity of air, and P denotes the hourly precipitation (mm h^{-1}).

3. Results

C. Meteorological data

For an accurate simulation of temperature conditions in the lake, using high-quality input data describing the meteorological conditions above the lake is crucial. These data directly affect the energy balance of the water surface and, consequently, the temperature conditions of the lake. This chapter presents measurements of key meteorological parameters that serve as input data for the 1D lake temperature model. Figure 1 presents the time series of meteorological data over the course of a year.

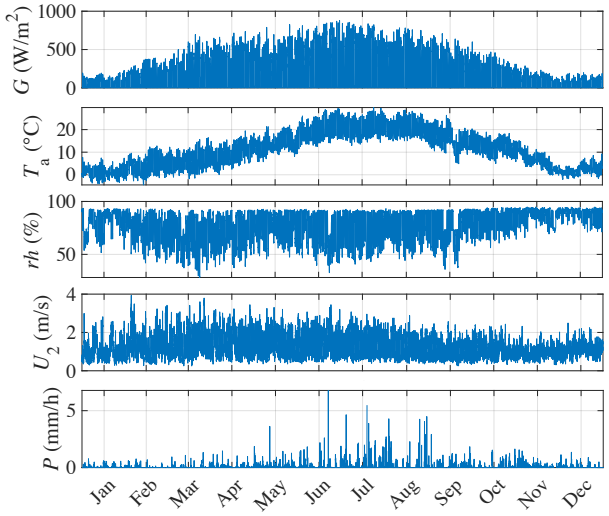

Fig.1. Time series of meteorological data over the course of a year.

Figure 1 shows meteorological data collected from 2019 to 2023. Annual averages were used to minimize the influence of short-term weather extremes. This approach provides a more representative description by reducing the impact of short-term extreme weather events and annual variations that may arise due to exceptional individual years. As a result, a more stable basis for modeling lake temperature conditions is ensured, minimizing the influence of specific climatic anomalies in individual years. The considered data include the power density of solar radiation G, ambient temperature T_a, wind speed at 2 m height U_2, relative humidity rh, and precipitation. These parameters are essential for properly modeling the energy exchange between the atmosphere and the water surface and assessing the impact of external meteorological factors on the lake's thermodynamics. The FPV system features an A-frame, pitched-roof structure. A 10 cm gap is maintained between PV modules to allow partial light penetration to the lake surface. Adjusting the spacing between individual modules influences the amount of solar radiation directly reaching the lake surface, thereby mitigating the potential shading effect of the floating PV system. To assess this impact, four different deployment scenarios of the FPV system on the lake will be presented, focusing on surface coverage and its effect on temperature variations. Figures 2 to 4 show the lake's temperature distribution across different depths under various conditions: without the FPV system, with FPV at different coverage levels, and the temperature differences between the scenarios with and without FPV. Temperature difference plots (ΔT) are shown using a diverging color scale, where blue indicates cooling and red indicates slight warming of the water column. The scale emphasizes seasonal and depth-dependent variations due to FPV coverage.

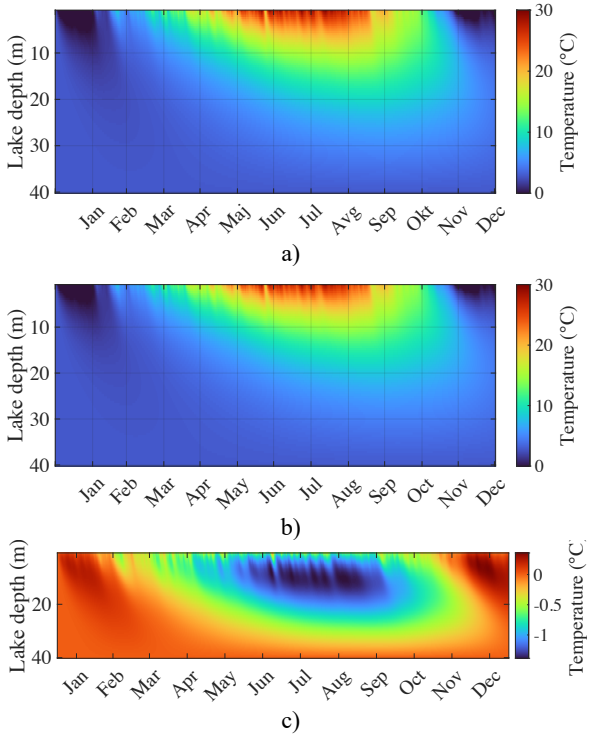

Fig.2. Temperature distribution of the lake: a) without the FPV system, b) with the FPV system (PV coverage = 25 %), and c) temperature difference ΔT.

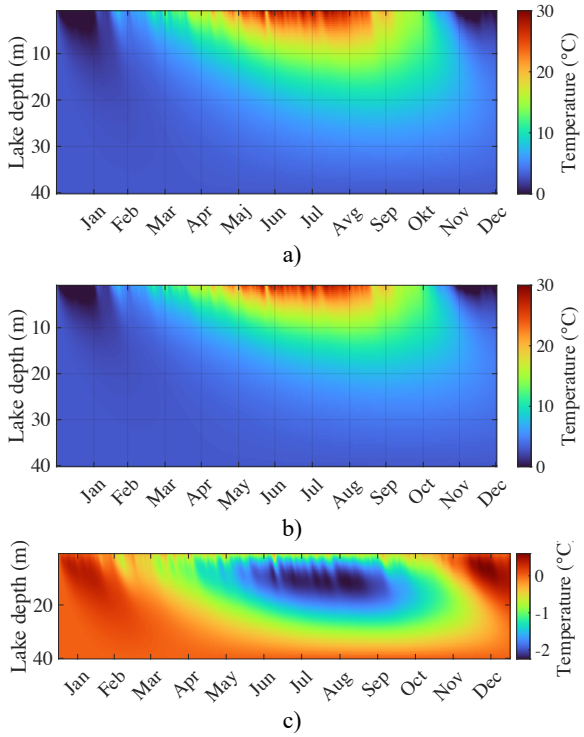

Fig.3. Temperature distribution of the lake: a) without the FPV system, b) with the FPV system (PV coverage = 50 %), and c) temperature difference ΔT.

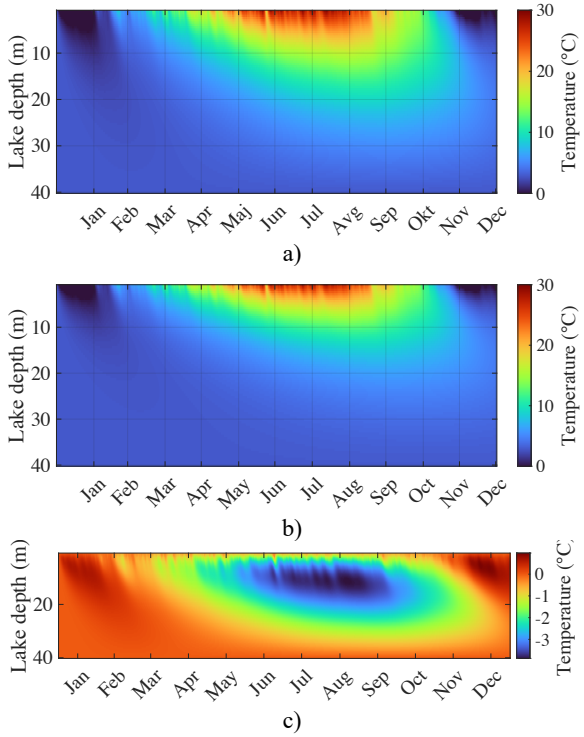

Fig.4. Temperature distribution of the lake: a) without the FPV system, b) with the FPV system (PV coverage = 75 %), and c) temperature difference ΔT.

Figures 2 to 4 show that the largest temperature differences ΔT occur during the summer months, particularly at depths between 2 m and 10 m, ranging from -1.38 °C to -3.80 °C, depending on the FPV coverage. The negative sign of ΔT indicates that the lake temperature with FPV is lower than that without FPV and vice versa. For a more detailed analysis, Tables 1 to 3 present the maximum and minimum temperature differences ΔT for different depths under varying FPV coverage (25 % to 75 %).

Table I. – Temperature differences (ΔT) at different depths with 75 % FPV coverage.

	FPV coverage 75 %	
depth	Minimum ΔT	Maximum ΔT
0.5 m	-0.92 °C (June)	0.18 °C (December)
0.5–2 m	-2.27 °C (June)	0.71 °C (December)
2–5 m	-3.30 °C (June)	0.97 °C (December
5–10 m	-3.80 °C (June)	0.96 °C (December)
30–40 m	-1.39 °C (September)	0.13 °C (February)

Table II. – Temperature differences (ΔT) at different depths with 50 % FPV coverage.

	FPV coverage 50 %	
depth	Minimum ΔT	Maximum ΔT
0.5 m	-0.92 °C (June)	0.18 °C (December)
0.5–2 m	-1.53 °C (June)	0.44 °C (December)
2–5 m	-2.00 °C (June)	0.60 °C (December
5–10 m	-2.24 °C (August)	0.60 °C (December)
30–40 m	-0.86 °C (September)	0.09 °C (February)

Table III. – Temperature differences (ΔT) at different depths with 25 % FPV coverage.

	FPV coverage 25 %	
depth	Minimum ΔT	Maximum ΔT
0.5 m	-0.92 °C (June)	0.18 °C (December)
0.5–2 m	-1.14 °C (June)	0.29 °C (December)
2–5 m	-1.32 °C (June)	0.35 °C (December
5–10 m	-1.38 °C (August)	0.35 °C (December)
30–40 m	-0.52 °C (September)	0.05 °C (February)

Tables 1 to 3 show that the FPV system significantly impacts the lake's thermal regime, with temperature changes depending on FPV coverage percentage and depth. During summer months (June–August), FPV induces cooling, particularly in the middle water layers (2–10 m), where the most pronounced temperature decreases of -3.80 °C occurred at 5–10 m with 75 % coverage in June. As FPV coverage decreases, the cooling effect becomes less pronounced. In contrast, during winter months (December–February), FPV reduces heat loss, resulting in slight warming, most notably at 2–5 m, where a 0.97 °C increase was recorded in December at 75 % coverage. The impact of FPV diminishes with depth, as the deepest layers (30–40 m) exhibit minimal temperature variations across all scenarios. These results suggest that FPV influences seasonal temperature distribution and vertical stratification, potentially affecting mixing processes and overall thermal stability.

4. Conclusion

This paper aimed to assess the impact of the FPV system on lake temperature using a 1D thermal model. The results show that FPV affects the thermal regime of the lake, with temperature changes depending on FPV coverage and depth. In summer, FPV induces cooling, with the most significant decrease observed at 5–10 m

(up to -3.80 °C at 75 % coverage). In winter, FPV reduces heat loss and limits evaporation by decreasing latent heat flux, leading to slight warming, particularly at 2–5 m (up to 0.97 °C in December). The reduction in evaporation during colder months further contributes to heat retention in the lake, affecting seasonal energy balance. The effect diminishes with depth, with minimal variations at 30–40 m. These findings highlight the influence of FPV on seasonal temperature distribution and stratification, emphasizing the need for site-specific assessments to optimize FPV deployment while considering potential environmental impacts.

The results of this paper, showing a summer cooling of up to –3.80 °C at 5–10 m depth and a winter warming of up to 0.97 °C, are consistent with findings by Ilgen et al. [8], who reported a surface cooling of up to –2.8 °C due to FPV deployment. Similarly, Yang et al. [11] observed a localized warming of approximately +0.3 °C under FPV structures, which aligns with the moderate winter heat retention reported here.

It should be noted, however, that the applied model includes certain simplifications. Assumptions related to turbulence and vertical mixing are generalized and may not fully capture transient stratification during changing weather conditions. Cloud cover is represented through averaged input data, which can limit the model's responsiveness to short-term variability in solar radiation. Furthermore, long-term thermal equilibrium is assumed, which may not reflect cumulative thermal feedback over extended periods. These factors should be considered when interpreting the results, particularly in the context of long-term planning and environmental assessment.

Acknowledgement

The authors acknowledge the use of research equipment DC power supply system for simulations of diffuse sources with an equipment set for managing energy systems together with a hybrid solar system, procured within the operation "Upgrading national research infrastructures – RIUM", which was co-financed by the Republic of Slovenia and the European Union from the European Regional Development Fund.

This APC was funded by the Slovenian Research Agency under grants Control of electromechanical systems P2-0115.

References

[1] X. Wang, W. Wang, Y. He, S. Zhang, W. Huang, R. I. Woolway, K. Shi, and X. Yang, "Numerical simulation of thermal stratification in Lake Qiandaohu using an improved WRF-Lake model", Journal of Hydrology (2023), Vol. 618, pp. 129184

[2] K. Šarović, M. Burić, and Z. B. Klaić, "SIMO v1.0: simplified model of the vertical temperature profile in a small, warm, monomictic lake", Geoscientific Model Development (2022), Vol. 15, pp. 8349–8375.

[3] R. Gaillard, M. Perroud, S. Goyette, and J. Kasparian, "Multi-column modelling of Lake Geneva for climate applications", Scientific Reports (2022), Vol. 12, pp. 353.

[4] H. Gu, B. Lu, C. Qi, S. Xiong, W. Shen, and L. Ma, "Water Temperature Simulation in a Tropical Lake in South China", Water (2021), Vol. 13, pp. 913.

[5] B. Tasnim, X. Fang, and J. S. Hayworth, "One- and Three-Dimensional Hydrodynamic, Water Temperature, and Dissolved Oxygen Modeling Comparison", Water (2024), Vol. 16, pp. 317.

[6] G. Exley, A. Armstrong, T. Page, and I. D. Jones, "Floating photovoltaics could mitigate climate change impacts on water body temperature and stratification," Solar Energy, vol. 219, pp. 24–33, 2021.

[7] Z. Liu, C. Ma, Y. Yang, X. Li, H. Gou, A. M. Folkard, "Water temperature and energy balance of floating photovoltaic construction water area—field study and modelling", Journal of Environmental Management (2024), Vol. 365, pp. 121494.

[8] K. Ilgen, D. Schindler, S. Wieland, J. Lange, "The impact of floating photovoltaic power plants on lake water temperature and stratification", Scientific Reports (2023), Vol. 13, pp 7932.

[9] P. Yang, L. H.C. Chua, K.N. Irvine, J. Imberger, "Radiation and energy budget dynamics associated with a floating photovoltaic system", Water Research (2021), Vol. 206, pp. 117745.

[10] M. A. Rahaman, T. L. Chambers, A. Fekih, G. Wiecheteck, G. Carranza, G. R. Collere Possetti, "Floating photovoltaic module temperature estimation: Modeling and comparison", Renewable Energy (2023), Vol. 208, pp. 162–180.

[11] P. Yang, L. H.C. Chua, K. N. Irvine, M. T. Nguyen, E. W. Low, "Impacts of a floating photovoltaic system on temperature and water quality in a shallow tropical reservoir", Limnology (2022), Vol. 23, pp. 441–454.